Synergetic muti-wavelength remote sensing versus *a posteriori* combination of retrieved products: Application for the retrieval of atmospheric profiles using MetOp measurements

Filipe Aires *

Laboratoire de Météorologie Dynamique / IPSL / CNRS, Université de Paris VI/Jussieu, France;

and Estellus SAS, France;

also associate to:

Laboratoire de l'Etude du Rayonnement et de la Matière en Astrophysique, CNRS, Observatoire de Paris, France

Ouahid Aznay

Laboratoire de Météorologie Dynamique / IPSL / CNRS, Université de Paris VI/Jussieu, France

Catherine Prigent

Laboratoire de l'Etude du Rayonnement et de la Matière en Astrophysique, CNRS, Observatoire de Paris, France

Maxime Paul

Laboratoire de l'Etude du Rayonnement et de la Matière en Astrophysique, Université de Paris VI/Jussieu, CNRS, Observatoire de Paris, France

Frédéric Bernardo

Institut Pierre-Simon-Laplace, Université de Paris VI/Jussieu, France

Raymond Armante, and Cyril Crevoisier

Laboratoire de Météorologie Dynamique / IPSL / CNRS, Université de Paris VI/Jussieu, France

ABSTRACT

In this paper, synergy refers to a process where the use of multiple satellite observations makes the retrieval more precise than the best individual retrieval. Two general strategies can be used in order to use multi-wavelength observations in an inversion scheme: First, the multi-wavelength observations are merged in the input of the retrieval scheme. This means that the various satellite observations are used simultaneously and that their possible interactions can be exploited by the retrieval scheme. Second, each multi-wavelength observations are used independently to retrieve a same geophysical variable and then, these independent retrievals are combined *a posteriori* using a simple weighted averaging for example. In this paper, it is shown that the first approach provides better synergy results because the retrieval process is able, in this case, to exploit the possible interactions between the various input informations. Since all the information is provided at the same time to the retrieval process, it is better suited to optimize their grobal use.
The two retrieval approaches are tested and compared using an application for the retrieval of atmospheric profiles and integrated column quantities (water vapour, ozone and temperature) using MetOp observations from IASI, AMSU-A and MHS instruments. The infrared and microwave observations appear to have a good retrieval synergy for atmospheric temperature, water vapour, and, surprisingly, for ozone thanks to the indirect synergy.

1. Introduction

Synergy refers to a process where the use of multiple satellite observations makes the retrieval more precise than the best individual retrieval. In (Aires 2011), it has been shown that various synergy mechanisms exist: (1) additive synergy, the simpler mechanism, where the addition of multiple informations on a same geophysical variable increases naturally the retrieval accuracy. (2) Indirect synergy, where the relationships between the geophysical variables are exploited by the retrieval scheme. (3) The non-linear synergy acts when interaction terms of the satellite

observations are relevant for the retrieval. (4) De-noising synergy refers to situations where the instrument noise of the observations are correlated in some sort. All these synergy mechanisms make the simultaneous use of all the observations beneficial for the retrieval with results more performant than the best individual retrieval.

It was shown in (Aires 2011) that the NN inversion model is particularly well adapted to exploit the synergy among satellite observations. In (Aires et al. 2011b), the InfraRed (IR) + MicroWave (MW) synergy from MetOp observations was tested for the retrieval of atmospheric temperature and water vapour profiles. These tests were performed using "theoretical" data from Radiative Transfer (RT) simulations.

In this paper, real observations will be used instead of the RT simulations: from IASI (Infrared Atmospheric Sounding Interferometer), AMSU-A (Advanced Microwave Sounding Unit-A) and MHS (Microwave Humidity Sounder) instruments. Furthermore, the retrieval scheme will retrieve atmospheric profiles not only for temperature and water vapour, but also for ozone. The total column amount of water vapour and ozone will be retrieved too. The IR and MW observations appear to have a good retrieval synergy for atmospheric temperature, water vapour, and, surprisingly, for ozone too.

Two general strategies can be used in order to use multi-wavelength observations in an inversion scheme: First, the multi-wavelength observations are merged in the input of the retrieval scheme. This means that the various satellite observations are used together and simultaneously by the retrieval scheme. Second, each multi-wavelength observations are used independently to retrieve a same geophysical variable and then, these independent retrievals are combined *a posteriori* for example using a simple weighted averaging. It will be shown that the first approach provides better synergy results because the retrieval process is able, in this case, to exploit the possible interactions between the various input informations. Since all the information is provided at the same time to the retrieval process, it is better suited to optimize their global use.

First, the datasets used in this study will be described, along with the necessary pre-processing of the data (section 2). A preliminary analysis of the satellite observations information content will be conducted in section 3. The retrieval methodologies and synergy measres are presented in section 4. The results will be described in section 5 using real observations. The retrieval of both integrated quantities and profiles will be assessed. Finally, section 6 will conclude this study and present the perspectives of this work.

2. Datasets

a. The satellite observations

Launched on October 19, 2006, MetOp is Europe's first polar-orbiting satellite dedicated to operational meteorology. It is a series of three satellites to be launched sequentially over 14 years, forming the space segment of EUMETSAT's Polar System (EPS). MetOp carries a set of "heritage" instruments provided by the United States and a new generation of European instruments that offer improved remote sensing capabilities to both meteorologists and climatologists. The new instruments increase the accuracy of temperature humidity measurements, wind speed and direction, and atmospheric ozone profiles. MetOp flies in a polar orbit corresponding to local "morning".

In this study, the observations from the following instruments will be used. The AMSU-A measures the oxygen band between 50 and 60 GHz, for the retrieval of atmospheric temperature profiles (Mo 1996). It is a cross-track scanning radiometer, with $\pm 48.3°$ from nadir with a total of 30 Earth fields-of-view of $3.3°$ per scan line, providing a nominal spatial resolution of 48 km at nadir. The instrument completes one scan every 8 seconds. The swath width is approximately 2000 km. AMSU-A is divided into two separate modules:

- AMSU Module A-1 with channels 3 to 15: 12 sounding channels in the 55 GHz O_2 band and one at the 89-GHz window;
- AMSU Module A-2 with channels 1 and 2 at 23.8 and 31.4 GHz.

AMSU-A is used in conjunction with the High-resolution Infrared Sounder instrument to estimate the global atmospheric temperature and humidity profiles from the surface to the upper stratosphere ($\simeq$50 km). AMSU-A measurements also provide precipitation and surface information including snow cover, sea-ice concentration and soil moisture.

The MHS is designed to measure the atmospheric water vapour profile, with 3 channels in the H_2O line at 183.31 GHz plus two window channels at 89 and 150 GHz (Hewison and Saunders 1996). MHS scans the Earth from left to right, in a vertical plane. Each swath is made up of 90 contiguous individual pixels sampled every 2.67 seconds. The scan is also synchronized with the AMSU-A1 and A2 instruments.

IASI is a state-of-the-art Fourier transform spectrometer based on a Michelson interferometer coupled to an integrated imaging system that observes and measures infrared radiation emitted from the Earth (Chalon et al. 2001). It has been developed by the French space agency CNES. The optical interferometry process offers fine spectral samplings of the atmosphere in the infrared band between the 3.2

and 15.5 microns representing 8461 channels. This enables the instrument to retrieve temperature and water vapour profiles in the troposphere and the lower stratosphere, as well as measure concentrations of ozone, carbon monoxide, methane and other compounds. For optimum operation, the IASI measurement cycle is synchronized with that of the AMSU-A1 and A2 (Advanced Microwave Sounding Units). This instrument was designed to reach accuracies of 1 K in temperature and 10% in water vapour with vertical resolutions of 1 km and 2 km respectively for cloud-free scenes. The signal-to-noise of IASI third band (2000-2780 cm^{-1}) is too low (measured radiance are low, and instrument noise is too high) and these channels cannot been used: only the first 5000 channels of the first two bands are used in the following.

The volume of data is very important because of the 8461 channels of IASI. In order to sample as well as possible the seasonal variability while keeping the volume of data reasonable, four weeks of data have been gathered: January, April, July, and October 2008. The datasets that we extracted have a global coverage, but in order to limit practical difficulties (space memory, computing time and sea-ice mask), only pixels from $\pm 30°$ in latitude have been kept in the experiments. This spatial limitation doesn't reduce the generality of the following results.

It has been shown in (**?**) and (Aires et al. 2011b) that it is very important, before applying the retrieval algorithm, to preprocess the IASI data using a Principal Component Analysis (PCA). This is usefull to compress the data, and also to reduce the instrument noise. In order to process the observations of the two wavelengths considered (MW and IR) in a systematic way, we have also used a PCA for the MW observations. Based on the percentage of variance explained by each PCA components, we selected 20 components for IASI and 12 for MW. This is a rough estimate of the number of independent pieces of information that can be extracted from each wavelenghts.

b. The ECMWF analyses

The atmospheric profiles and surface properties from the 6-hourly operational global analyses from the Integrated Forecasting System (IFS) of the European Center for Medium Range Forecasting (ECMWF) (**?**) are used in this study. The following information is kept: the temperature, water vapour (relative humidity in % hereafter) and ozone profiles on 43 pressure levels ranging from 1000 to 1 hPa (these levels have been interpolated for the inital 21 levels in order to be used with the RTTOV code). These analyses are provided on a regular $1.125° \times 1.125°$ grid, every six hours.

The higher-level layers have no real variability and there is no reason to maintain them in our retrieval scheme and a selection had to be made: (1) All the levels are kept for the temperature retrievals; (2) The five highest atmospheric layers are suppressed for the water vapour (higher than 10 hPa); (3) And the eight highest layers are suppressed for the retrieval of ozone (higher than 50 hPa). The cloud cover information from the ECMWF analysis is also kept, to filter out in our retrieval process the cloudy scenes.

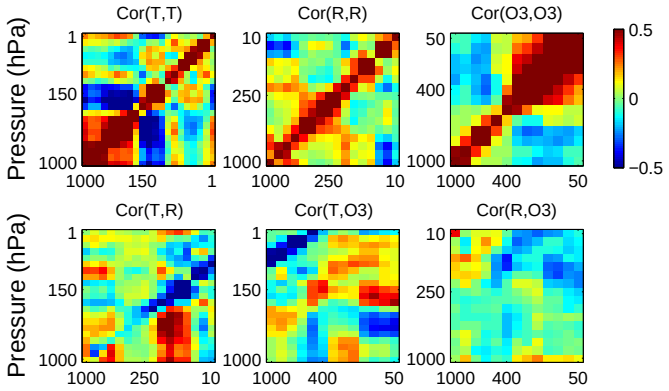

FIG. 1. Top: Auto-correlation matrices for atmospheric profiles of (from left to right) Temperature (T), Relative humidity (R), and Ozone (O3). Bottom: Correlations among the atmospheric profiles (from left to right): T & R, T & O3 and R & O3.

Fig. 1 represents the correlations between the geophysical atmospheric profiles, among themselves (Top) and between them (Bottom). It can be seen that the vertical correlations for temperature are stronger for temperature than for water vapour. The ozone has a strong vertical correlation in the upper troposphere, where the ozone content is higher. The correlation between the profiles indicate that the temperature profile is strongly correlated to the water vapour for pressures higher than 250 hPa. There exist also a strong correlation between the temperature and ozone for both surface and upper layers. The correlation between water vapour and ozone is less important but it is still significant.

c. The aerosols

A climatology of aerosols in some *in situ* locations has been obtained from AERONET stations. AERONET is a globally distributed network of automated ground-based instruments and data archive system, developed to support the aerosol community. The instruments used are CIMEL spectral radiometers that measure the spectral extinction of the direct Sun radiance (Holben *et al.*, 1998). The Aerosol Optical Thicknesses (AOTs) are determined using the Beer-Bouguer Law in several spectral bands. For this study, level-2 data are used and consist of AOTs at 440 nm, 675 nm and 870 nm retrieved at least every 15 mn during day time. Level-2 data are cloud-free and qual-

ity assured retrieved from pre- and post-field calibrated measurements (Smirnov et al. 2000). The estimated accuracy in the AERONET AOTs is between ±0.01 and ±0.02 depending on the wavelength, for an airmass equal to 1 (Dubovik *et al.*, 2000).

A spatial interpolation scheme has been applied to obtain AOT fields at a horizontal resolution of 1.125°×1.125° (same as the ECMWF analyses). This spatial interpolation scheme is rather crude (a bilinear interpolation). In order to obtain better AOT fields, a dedicated interpolation scheme would have to be developed specifically for AOT fields. This could be based for example on a PCA of AOT fields but since such a dataset is not available, this approach cannot be used here. The alternative would be to develop an AOT retrieval scheme based on the satellite observations, but this is beyond the scope of this study. This aerosol information is used to identify the optical thickness regime of each particular scene. This is important for the IR observations.

d. Spatio-temporal coincidences

The satellite observations have to be matched in space-time coincidence. The three instruments being onboard the same satellite, good coincidences are obtained. The collocation of the MW observations is easy, the instruments have been designed to facilitate this step: each AMSU-A pixel is associated to the corresponding 3×3 higher resolution pixels of MHS. The MW observations are then projected into the IASI pixels using a closer pixel rule. The final resolution of the dataset is the IASI resolution.

The aerosol information presented in section c is projected in the 1.125° × 1.125° regular grid of the ECMWF analysis data of section b. This analysis and aerosol dataset is then projected into the satellite observations. A time threshold of 30 mn is used for this collocation, only some of the satellite orbits are kept around the analysis time steps at 0, 6, 12 and 18 h UTC. For each satellite pixel, the closest analysis grid point is taken, this means that there can be multiple use of the same analysis grid cell).

Only oceanic situations are kept. The total cloud cover for the ECMWF is used to reject all the cloudy situations.

3. Preliminary analysis

a. Sensitivity analysis

The Jacobian of the RTM are estimated for the three instruments that are considered here, namely AMSU-A, MHS and IASI. RTTOV radiative transfer model provides analytical Jacobians. However, for practical reasons linked to computational time, the Jacobians are estimated using RTM simulations on perturbed input profiles. The perturbations are chosen to be 1 K for temperature and 10 % for relative humidity and ozone (in PPMV) (Please, see (Garand and et Al. 2001) for an intercomparison study of such Jacobians). Figures 2, 3 represent respectively the

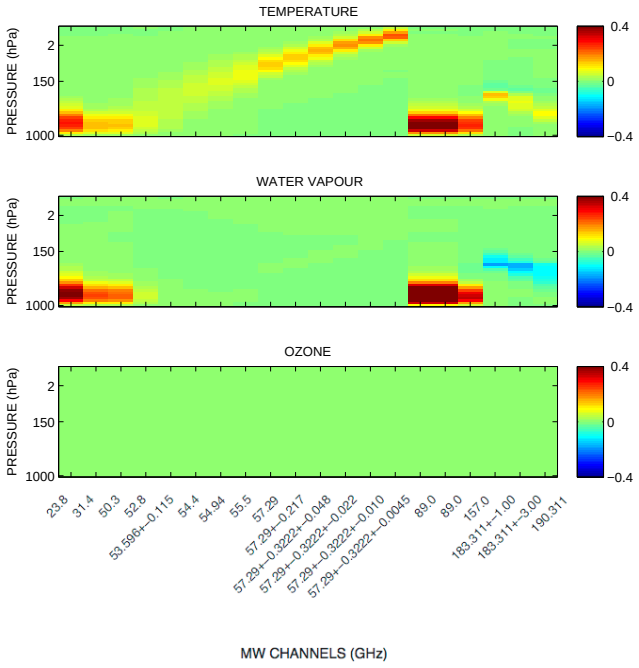

FIG. 2. Jacobian of the AMSU-A+MHS observations with respect to temperature (Top), water vapour (Middle), and ozone (Bottom) atmospheric profils for a typical ocean scene over the Tropics.

temperature, humidity and ozone Jacobians for AMSU-A, MHS, and IASI for a typical Tropical situation over the ocean. It appears that MHS instrument is as expected more sensitive to changes in relative humidity than to changes in temperature. AMSU-A provides information nicely spread in the vertical. Its window channels are sensitive to both temperature and water vapour. MHS provides a better vertical coverage for water vapour. As expected, there is no sensitivity to ozone in the MW observations. COMMENTER IASI (15 micron pour temperature, et water vapour)

The magnitudes of Jacobians are comparable for the three instruments, including the infrared from IASI. However, the vertical resolution for IASI is higher for water vapour in the upper troposphere, and for the temperature for the whole troposphere. Furthermore, the IASI instrument possesses a lot of channels, this has a lot of consequences for the retrievals (i.e., computation time for the retrieval, necessity to perfrom a dimension reduction on the observed spectra, redundancy considerations for the de-noising, etc.).

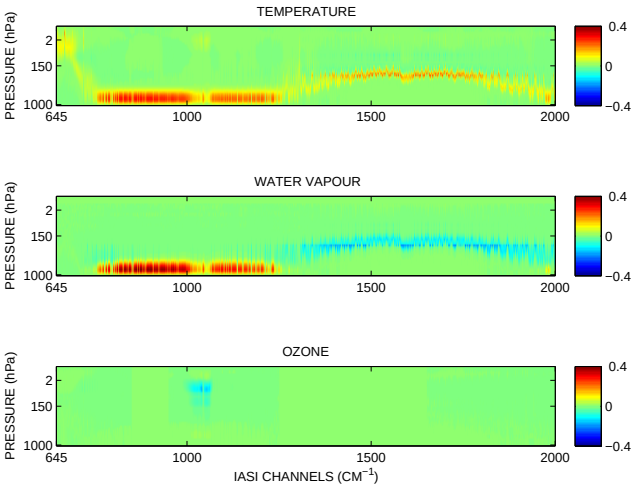

FIG. 3. Jacobian of the IASI observations with respect to temperature (Top), water vapour (Middle), and ozone (Bottom) atmospheric profils for a typical ocean scene over the Tropics for the first two band of IASI.

b. Correlation matrix analysis

The correlation matrices between the temperature, water vapour and ozone atmospheric profiles with respect to the observations in the MW, respectively IR are represented in Fig. 4, respectively Fig. 5. These correlation matrices using real observations provide a good and simple information content analysis. They can be related to the sensitivity of the observations to the geophysical parameter of interest, but also to the correlation of the observations with a parameter that is itself correlated to the parameter of interest (indirect synergy).

For instance, let us examine the correlation between the microwave observations and the water vapour. The major water vapour line is located at 183 GHz, with a much weaker line at 22 GHz. Outside these two lines, the contribution of the water vapour continuum increases with the frequencies. One would expect that the correlation between the observations and the water vapour to be higher (in absolute value) in the absorption lines, and to increase with the continuum absorption. For pressures below 200 hPa, the amount of water vapour is limited and correlation structures between the water vapour and the observations in the H_20 lines or in window channels are very likely related to the correlation of the water vapour between the different levels in the ECMWF analysis. From the analysis of the Jacobian in water vapor, we saw that the sensitivity to water vapor was high in the 183 GHz channel but very low in the O_2 band aroud 60 GHz. The correlation with the observations in the O_2 band is to be attributed not to the sensitivity of the Tbs to the water vapor directly but to the correlation between the water vapour with the temperature. Note that the correlation with the temperature and with the water vapour shows rather similar patterns (top and middle figure), in relation with the correlation between water vapour and temperature. By the same token, the microwave observations are not expected to be sensitive to the ozone variation. The correlation between the microwave observations and the ozone in the O2 band is actually due to the correlation between temperature and ozone, in the ECMWF reanalysis.

Similar conclusions can be derived for the infrared. The strong water vapour band above 1500 cm^{-1} induces large correlation between the observations and the water vapour. This frequency band is also very correlated to the temperature, as expected from the analysis of the Jacobians in temperature. In the CO_2 absorption band, the correlation between the IASI observations above 645 cm^{-1} and the temperature is large, negative in the lower atmosphere and positive in the higher atmosphere, related to the inversion in temperature in the atmosphere. As a consequence, a 1D-var retrieval scheme that uses the Jacobians is expected to have a different behavior, than a statistical retrieval method such as the NNs.

We also observe large correlation in this frequency range with the water vapour and the ozone, due to the intrinsic correlation between the three atmospheric variables in the atmospheric profiles. The O_3 band above 1000 cm^{-1} induces similar effect on the water vapour and temperature.

The retrieval methodologies is trained on the database of satellite observations and coincident ECMWF atmospheric profiles. We have to keep in mind that it will not only exploit the direct sensitivity of the observations to the selected atmospheric parameter, but also benefit from the correlation between the different variables at the different levels, and from the correlation of the given variable along the vertical. We also have to be aware that limitation in the atmospheric profiles such as the one pointed out for ozone can limit the quality of the retrieval for this variable.

4. Retrieval methodology

a. Architecture of the neural network inversion models

NN techniques have proved very successful in developing computationally efficient remote sensing algorithms. The Multi-Layered Perceptron (MLP) model (Rumelhart et al. 1986) is selected here. It is a non-linear mapping model: given an input TB (i.e., the satellite observations), it provides an output f (i.e., the geophysical variables to retrieve) in a non-linear way. In this paper, a NN model with only one hidden layer will be considered. The MLP model is defined by the number of input neurons (i.e., the size of the inputs, number of channels), the number of ouputs (i.e., the size of the geophysical variables to retrieve) and the number of neurons in the hidden layers that control the complexity of the model. A study has to be

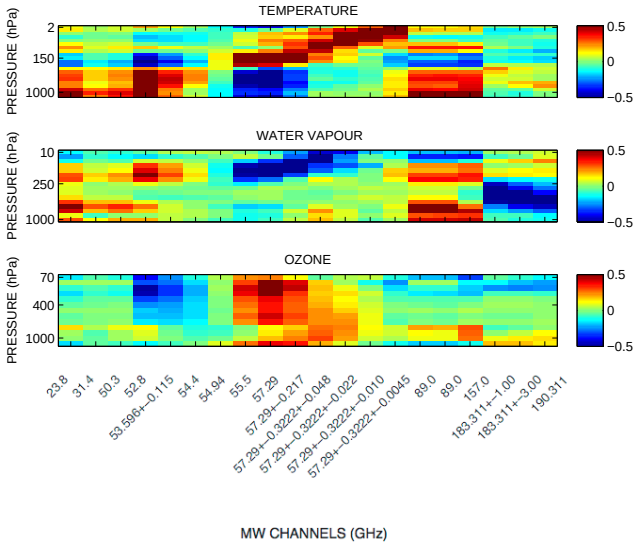

FIG. 4. Correlations between AMSU-A and MHS observations and the ECMWF atmospheric profiles of temperature, water vapour and ozone.

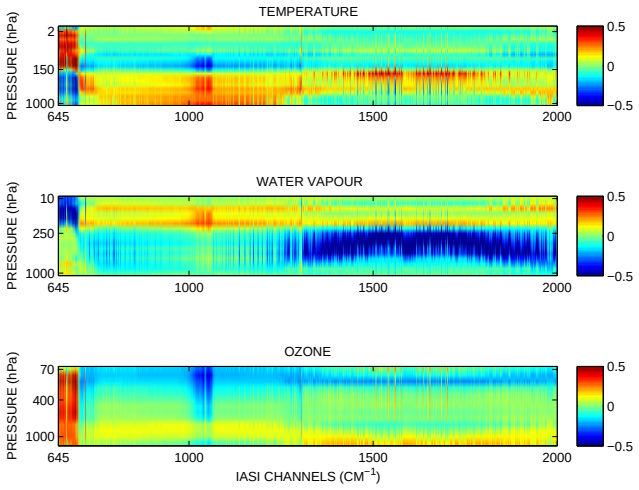

FIG. 5. Correlations between IASI observations and the ECMWF atmospheric profiles of temperature, water vapour and ozone.

Configuration	Number of inputs	Hidden neurons	Number of outputs
Temp-IASI	20	20	21
Temp-MW	12	20	21
Temp-IR+MW	32	25	21
WV-IASI	20	20	16
WV-MW	12	20	16
WV-IR+MW	32	25	16
O_3-IASI	20	20	13
O_3-MW	12	20	13
O_3-IR+MW	32	25	13

TABLE 1. Architecture of the NN retrieval models

conducted to define the optimal number of neurons in the hidden layer. A balance needs to be found: Too many free parameters in the model can conduct to the over-learning (over-parameterization) leading to degraded generalization properties. On the contrary, too few free parameters will yield under-parameterization and bias error of the model. Table 1 represents the number of neurons in input, hidden and output layers for the various configuration that are used in this paper.

Since the NN performances will be compared using different numbers of inputs (only the IR, only the MW or both), it is important to address the relative stability of the training. A NN with more inputs will have more free parameters and more information to exploit; this can complexify the NN training, and the learning step can become much longer. An over-parameterization can led to over-training if the learning process is not regularized. Good testing and validation datasets, stopping criterion, and the multiple initialisation of the weights for the learning tend to reduce this problem. The following Tab. 1 indicates the major characteristics of the NN models used in this study: the number of neurons in input, hidden and output layers.

The NN is a remarkable model for information merging (Aires et al. 2011b). Terms such as $x_1 \cdot x_2$ are sometimes introduced in regression models $y = f(x_1, x_2)$ to allow for the interaction of two inputs. These interaction terms are non-linear and can directly be represented by NN architectures and their use is optimized during the learning process. Saturation effects also play an important role when data is combined: an output can be sensitive to an input for a particular range and to another input for a different range. In order to represent this behavior, saturation effects need to be used in the regression model. This is well represented by the sigmoid functions used by each neuron in the NN model.

b. The learning, testing, and validation datasets

The NN is trained to reproduce the behavior described by a database of samples composed of inputs (i.e., the real observions TBs) and their associated outputs (i.e., the geophysical variables f), for $e = 1, \ldots, N$ with N the number of samples in the training database. Provided that enough samples (TB^e,f^e) are available, any continuous relationship, as complex as it is, can be represented by a MLP (Hornik et al. 1989; Cybenko 1989).

A quality criterion that measures the discrepancies between the NN outputs and the desired targets from the learning dataset has to be defined. In this study, the outputs of the NN are the atmospheric profiles (temperature, water vapour and ozone) and integrated column quantities of water vapour (i.e. $TCWV$) and ozone (i.e. TCO_3). This quality criterion is minimized during the learning of the NN, it has to be carefully chosen.

The learning algorithm used to train the NN is the classical Back-Propagation algorithm. This optimization technique has long proved its efficiency for such problems.

Over the whole dataset of coincident real satellite observations and analyses, 60% are kept for the learning, 20% for the testing, and 20% for the validation. The training of the NN, i.e., the calibration of the retrieval scheme is performed on the learning dataset.

The testing dataset is used during the learning to test the NN results on data not directly used in the learning. This allows measuring the generalization capacity of the NN, i.e., its ability to perform retrievals on other data. During the learning, the generalization errors are monitored and the learning is stopped when, after a decrease, they start to increase. This procedure avoids the overtraining of the retrieval, i.e., the problem of an algorithm that performs very well on its learning dataset, but poorly on other data.

The testing dataset is used several times, first to measure the generalization capacities of the NN on each step of the learning process, second for all the tested NN configurations, and finally for all considered retrieval configurations (e.g., angle, optical thickness). As a consequence, the whole NN selection process could "learn" the testing dataset (i.e., be biased towards it) and the evaluation of the generalization errors could become misleading. To avoid this problem, another independent dataset is used: the validation dataset. It is only used to estimate the retrieval errors on an independent dataset, once the learning is done, and once the model is chosen.

c. Regime selection

The retrieval algorithm has been developed for various configurations:

- Viewing Zenith Angle equal to 0, 10, 20, 30 or 40°;
- Solar Zenith Angle equal to 40, 50 or 60°;
- Aerosol Optical Thickness equal to 0.0, 0.1 or 0.2;
- Land or ocean cases;
- Clear or cloudy situations.

This regime selection results in $5 \times 3 \times 3 \times 2 \times 2 = 180$ datasets designed to train 180 specialized retrieval schemes. However, only the clear cases over ocean are considered in the retrieval tests in this study. Furthermore, in order to limit the impact of the aerosols in the visible measurements, only AOT <0.05 are kept. As a consequence, a total of fifteen NNs have been trained.

d. Physical versus empirical retrievals

In order to train the NN, two strategies could be used:

- The inversion can be trained on a learning database composed of the atmospheric profiles from the ECMWF analysis, along with the simulated observations in the two wavelength ranges derived from RT calculations (instead of real observations). This type of inversion is said to be a "physical" inversion, as it uses a physical RT model. However, this second possibility requires a preliminary calibration step to insure that the RT simulations and the real observations are "compatible" (i.e., have similar statistics).
- The training can also be done using a learning database composed of the satellite observations and collocated profiles from ECMWF analysis. This type of scheme is said to be an "empirical" inversion because no RT model is used to solve the inverse problem.

The first approach involves explicitly two transformations, namely the calibration of the satellite data and the actual retrieval (Aires et al. 2010). The second approach involves only one transformation of the real observations: it mixes the calibration and the retrieval in a unique procedure. Both methods could lead to satisfactory results, but the second one is preferred here because obtaining a good calibration procedure for both the IR and MW is a particularly difficult task.

The use of the ECMWF analyses as the "truth" for the training of the Neural Networks (NNs) is justified because these analyses are the best knowledge of the state of the atmosphere and surface: all the available satellite observations, all the *in situ* measurements from the weather stations have been assimilated in the best weather/climate model.

e. Synergy measures

1) Synergy factor

A synergetic scheme refers to an algorithm that uses simultaneously or hierarchically the observations of two or

more spectral ranges in order to obtain a more accurate retrieval than the independent retrievals. We define a synergy factor of a retrieval scheme using R sources of information $(x_1, \ldots, x_R)$ (each one can be multivariate) as the ratio of the errors of the retrieval using the best single information, $\min_{i=1,\ldots,R} E(x_i)$ with the errors of the retrieval using all the sources of information, $E(x_1, \ldots, x_R)$. In terms of percentage of synergy, this corresponds to:

$$F_{\text{syn}} = 100 \cdot \left(\frac{\min_{i=1,\ldots,R} E(x_i)}{E(x_1, \ldots, x_R)} - 1 \right). \quad (1)$$

There is synergy when this ratio is positive. This synergy measure can be used for any type of algorithm, including the *a posteriori* combination of products described in the following section.

2) *A posteriori* combination versus synergetic data fusion

In this study, the goal is to merge synergeticaly the IR and MW observations directly as inputs to the retrieval algorithm. It is unusual to exploit such data fusion/merging strategy: In many retrieval schemes using multiple wavelength data, the independent retrievals from each instrument observation are, instead, combined *a posteriori*. An example of such *a posteriori* combination is given, for example, in Liu *et al.* (2011) where two soil moisture estimates from two different algorithms using passive and active microwave observations are simply averaged.

This *a posteriori* combination by simple averaging can be optimized, for example, by performing a weighted average based on the uncertainties of the two retrievals. This is what is done in optimal interpolation or the assimilation. Combining two independent retrievals f_{IR} and f_{MW} using IR and MW observations, each one with uncertainty estimates σ_{IR} and σ_{IR} is optimal when using:

$$\hat{f} = \frac{\sigma^2_{MW}}{\sigma^2_{IR} + \sigma^2_{MW}} \cdot f_{IR} + \frac{\sigma^2_{IR}}{\sigma^2_{IR} + \sigma^2_{MW}} \cdot f_{MW} \quad (2)$$

The theoretical uncertainty related to this estimator is given by:

$$\hat{\sigma} = \sqrt{\left(\frac{\sigma^2_{MW}}{\sigma^2_{IR} + \sigma^2_{MW}} \right)^2 \cdot \sigma^2_{IR} + \left(\frac{\sigma^2_{IR}}{\sigma^2_{IR} + \sigma^2_{MW}} \right)^2 \cdot \sigma^2_{MW}}. \quad (3)$$

This expression can be generalized when more than two sources of information are available. Other more sophisticated *a posteriori* combinations could also be considered, in particular, regime-dependent combinations which takes into account the state dependency of the individual retrieval uncertainties.

In the following, the results of the retrieval scheme that performs synergetic merging of the satellite observation in the inputs of the retrieval scheme will be compared to the results of this *a posteriori* combination of independent retrievals. The same amount of data is used in both of these approaches so it is very interesting to compare the results, in order to see if the merging of the satellite data can exploit the potential interactions among the observations.

5. Retrieval results

The retrieval of the atmospheric profils is first presented and the synergy factors are presented for each atmospheric layers. The retrieval of the integrated quantities ($TCWV$ and TCO_3) is then analyzed, in particular, investigating the *a posteriori* combination.

The retrieval statistics are provided for the following configuration: the aerosol content is low (between 0 and 0.05), Viewing Zenith Angle=40° but Solar Zenith Angle is composited for the various configurations (See subsection c). Note that similar results have been obtained for the other configurations. The tests are performed over ocean under clear sky conditions. Statistics are calculated using the validation dataset (i.e., data not used in the learning or generalization datasets), see section b.

a. Temperature, water vapour and ozone profiles

The statistics are provided for retrievals using only MW, only IR, or IR+MW observations. Fig. 6 represents the RMS for the retrieval of the atmospheric temperature profile. Surprisingly, the MW retrieval is better than the IR, especially in the lower troposphere, except in some layers around 300-100 hPa. REF JACOBIANS AND CORRELATIONS. The IR+MW data fusion, in the NN retrieval scheme, benefits from a strong synergy, with RMS ranging from 1 to 1.5 K in most atmospheric layers. The synergy estimations for these temperature profile retrievals will be analyzed in the following.

Similar statistical results are given in Fig. 7 for the retrieval of the atmospheric water vapour profile. The IR observations from IASI appear to be more informative than the MW measurements from MHS/AMSU-A. This is particularly true for the upper troposphere above 300 hPa. REF JACOBIANS AND CORRELATIONS. The IR+MW data fusion has statistics...

Since the profiles of ozone have very different ranges of variability in the lower or higher troposphere, it is more convenient to represent the standard error of the retrieval in terms of percentage of errors. It can be seen in Fig. 8 that errors are higher at high altitudes around 100 hPa (i.e. where the ozone content is higher) and near the surface (where the ozone content is really low). Except for few lower atmospheric layers, the IR from IASI provides the best information for the ozone profile retrieval. The synergy is very good when IR and MW are merged. The overall retrieval of the ozone atmospheric profile has a good

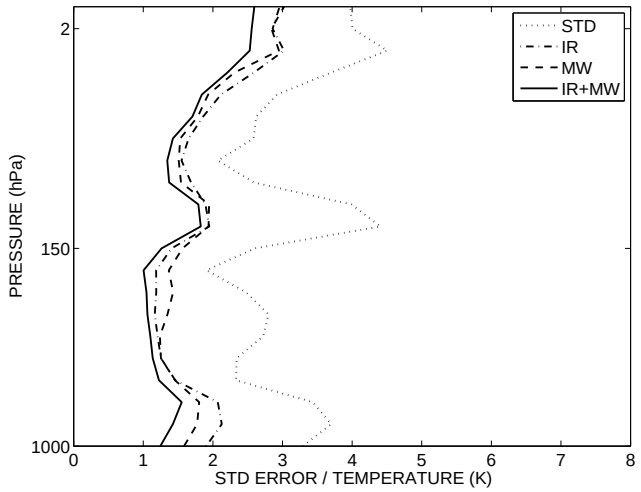

FIG. 6. Root Mean Square errors for the temperature retrievals from IASI (dot-dashed), MW (dashed), IR+MW (continuous) instruments. The natural STD of the temperature is also provided (in dotted line) for comparison purpose.

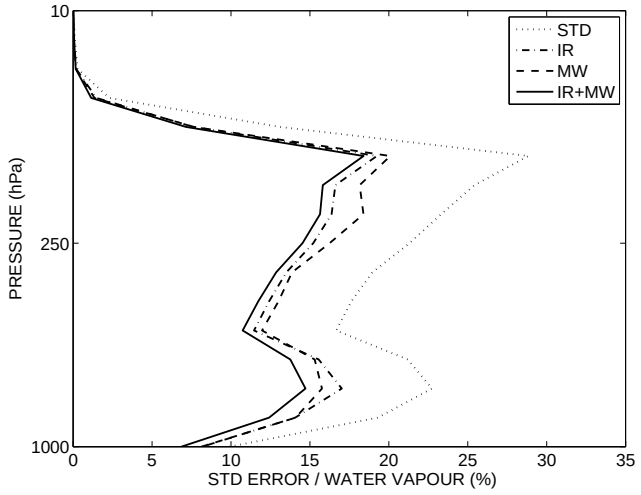

FIG. 7. Root Mean Square errors for the water vapour retrievals from IASI (dot-dashed), MW (dashed), IR+MW (continuous line) instruments. The natural STD of the temperature is also provided (in dotted line) for comparison purpose.

quality with levels lower than 30% and often lower than 15%. It should be noted, again, that our absolute uncertainty might be underestimated because the ozone profiles from the ECMWF analyses might be too simple compared to real profiles. Furthermore, this study focuses on $\pm 30^{\circ}$ in latitude, with possible limitations of the ozone variability in this region[1]. It is surprising that MW observations help improving the IR retrieval of ozone since it has been shown in the Jacobian study of section a that the MW measurements are not sensitive to ozone. However, it has been seen in section b that the MW brightness temperatures are correlated to the ozone profile (Fig. 4). This illustrates well that contrarily to a 1D-var inversion scheme that is based on the Jacobians, is not using the same information than a statistical retrieval scheme such as the NN that exploits the correlations.

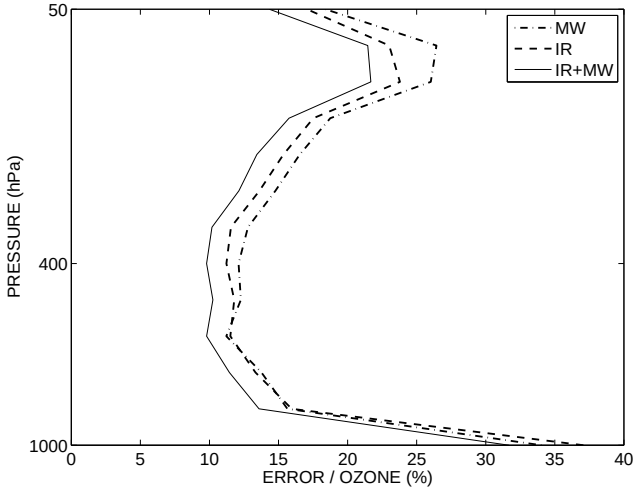

FIG. 8. Mean absolute errors, in percentage, for the ozone retrievals from MW (dot-dashed), IR (dashed), and IR+MW (continous line) observations.

Fig 9 represents the synergy measured when IR and MW observations are combined to retrieve temperature, water vapour and ozone atmospheric profiles. This synergy factor is based on Eq. (1). Synergy factor ranges from 10 to 15% for temperature for all the considered atmospheric layers. The synergy for the ozone has similar characteristics. The synergy for the WV is overall very interesting, between 5 and 15%, in agreement with the retrieval of $TCWV$ in section b. Water vapour is also positive for most atmospheric layers, except for the two top layers where it is known that low information content is provided by the satellite observations. Numerical instabilities can also be present.

[1]Please, note that the limitation of the range of variability of the variable to estimate is also a difficulty for the retrieval scheme

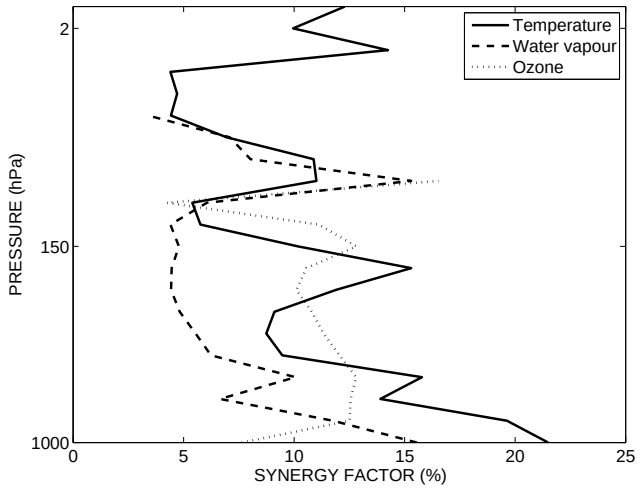

FIG. 9. Synergy statistics for the retrieval of the temperature (continuous), water vapour (dashed) and ozone (dotted) atmospheric profiles. The retrieval uses the IR, MW observations from AMSU-A, MHS and IASI instruments.

b. The integrated quantities

1) EVALUATION OF THE NEURAL NETWORK RETRIEVAL

In this section, the retrieval of the $TCWV$ and TCO_3 variables are performed using the data fusion/merging principle described in section 4: the NN model uses simultaneously the IR + MW observations to perform the retrieval.

Fig. 10 represents two scatterplots of the retrieved $TCWV$ (A, left) and TCO_3 (B, right) versus the target from the ECMWF analysis when various satellite observations are used (MW from AMSU-A and MHS, IR from IASI, and IR+MW/SYN (the IR+MW/WEI configuration will be commented in next section). The scatterplots indicate that the dispersion from the individual instrument retrievals (MW or IR) is higher than the scatter obtained with the IR+MW retrieval (in red). This general behavior is confirmed for both $TCWV$ and TCO_3.

The linear regression of the retrieval versus the target is also represented, with the same color code. The closer the linear regression to the diagonal (in black), the better the retrieval: it means that the natural damping of a statistically retrieved parameter is less of a problem. The best linear regression line is obtained with the IR+MW/SYN configuration (in red) meaning that synergy operates well.

The conclusions of these scatterplots are confirmed by the results presented in Tab. 2, correlation and synergy statistics are provided for both $TCWV$ and TCO_3, for the IR, MW, and IR+MW configurations.

The MW observations are the better information for the $TCWV$ (RMS=3.34 $kg.m^{-2}$), surprisingly better than the IR observations from IASI (RMS=4.53 $kg.m^{-1}$). However,

	IASI	MW	IR+MW
RMS error $TCWV$ (kg.m^{-2})	4.528	3.339	2.895
RMS error TCO_3 (DU)	6.588	8.198	4.872
Correlation $TCWV$	0.893	0.943	0.958
Correlation TCO_3	0.921	0.874	0.957
STD error TCO_3 (%)	2.6	3.2	1.9
Synergy $TCWV$ (%)			11.7
Synergy TCO_3 (%)			26.0

TABLE 2. RMS, correlation and synergy statistics for the retrieval of $TCWV$ and TCO_3 using IASI, MW, and IR+MW satellite observations.

it should be noted that the cloud flag that was used to filter the cloudy situations in this study is based on the total cloud cover from the ECMWF analysis (see section b) and this is far from a perfect cloud flag information. It has been seen, in previous section, that cloudy situations, affecting more the IR than the MW observations, contaminate our statistics. However, it is known in the NWP centers that the MW observations are very important for the quality of the weather forecast, more than the IR observations, and our results seem to converge to this statement for the $TCWV$. The data fusion of the IR and MW in our retrieval scheme results in a very interesting synergy factor, 11.7%, with an RMS=2.948 $kg.m^{-2}$. The correlation statistics follow these RMS statistics, the $TCWV$ retrieval in the IR+MW/SYN configuration has a 0.958 correlation with the target, which is a very good result.

For the retrieval of the TCO_3, the best information is provided by the IR observations from the IASI instrument (RMS=6.6 DU) followed by the MW (RMS=8.2 DU). This could be surprising considering that MW observations are not physically sensitive to O_3. However, the IR and MW numbers are very close. Furthermore, MW observations and O_3 content have shown strong correlations in Fig. 4. The MW appears to be linked to O_3 (correlation=0.874), but it is related to an indirect correlation: the MW is related to temperature and water vapour, and the temperature and water vapour are themselves related to O_3 in the ECMWF analysis. Our processing of the IR observations is not perfect (see sections b and c): the cloud and aerosol flags are not optimal and this is particularly a problem for the IR. The synergy obtained when IR and MW are used is impressive, equal to 26%, with a RMS down to 4.9 DU. The synergy operates even better for the TCO_3 than for the $TCWV$. The three instruments have a significant contribution when used together. The standard error for the retrieval of ozone is also provided in percentage, this is a common way to measure the quality of the ozone retrieval.

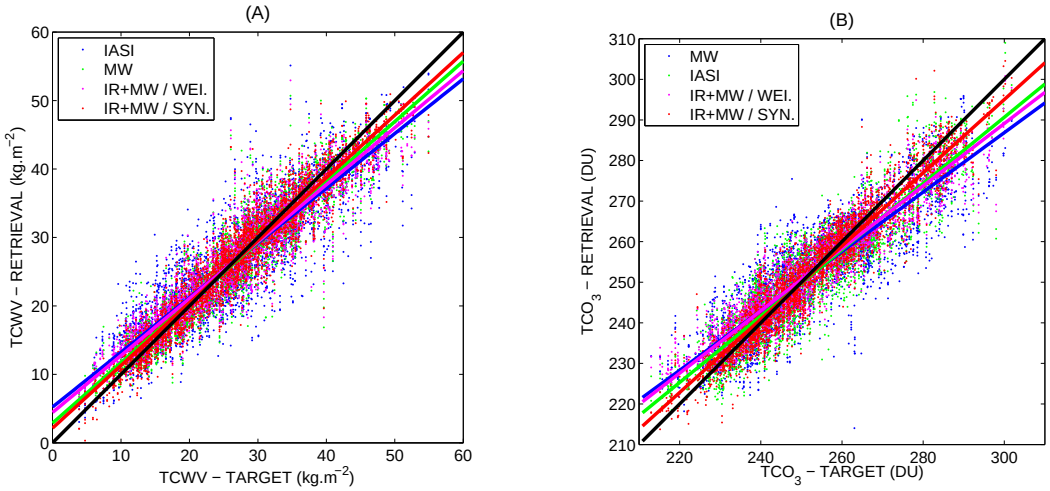

FIG. 10. Scatterplot of the retrieved versus target $TCWV$ (A, left) and TCO_3 (B, right) for IASI (blue), MW (magenta), IR+MW/WEIghted algorithm (magenta), IR+MW/SYNergy (red) retrievals. The linear regression of the scattered data for each one of the retrievals is also represented using the same color code.

2) SATELLITE DATA FUSION VERSUS *a posteriori* COMBINATION OF PRODUCTS

In this section, we investigate whether *a posteriori* combinations of products provides similar results than our satellite data merging. We will consider two *a posteriori* combinations: the simpler one where the two estimates from the IR and MW are averaged, and the weighted average that takes into account the uncertainty of each retrieval.

The scatterplots of the retrieved versus the target $TCWV$ (A, left) and TCO_3 (B, right), for the weighted *a posteriori* combination (in magenta) and the data fusion (in red) from the NN retrieval exploiting the IR+MW observations are represented in Fig. 10. The dispersion appears to be lower for the data fusion retrieval, for both the $TCWV$ and TCO_3. The linear regression of the data fusion is closer to the diagonal (in black) than the linear regression of the *a posteriori* combination, showing that the dynamics of the $TCWV$ and TCO_3 variables is better retrieved by the synergetic data fusion than by the *a posteriori* combination.

It is possible to estimate the theoretical retrieval uncertainties from these *a posteriori* combinations by using the individual uncertainties of the two independent retrievals (see Eq. (3)). These theoretical estimates are compared in Tab. 3 to the real retrieval from the simple and weighted averages *a posteriori* combinations, and to the NN retrieval in the IR+MW configuration. The synergy is also estimated in this Table for the real retrieval (not for the theoretical estimates).

First, it can be noted that the theoretical estimates (for both the simple and the weighted averages) are an underestimation of the real retrieval uncertainties: instead of 2.813 for the average or 2.687 for the weighted combination, the actual retrievals have respectively a retrieval uncertainty of 3.561 and 3.402 $kg.m^{-2}$ for $TCWV$. Similarly for the retrieval of TCO_3, the actual retrieval uncertainties 6.301 and 6.15 DU for the simple or weighted averages are significantly greater than the theoretical estimates (5.528 and 5.135). These significant differences prove that the assumptions to estimate the theoretical uncertainties are too simplistic: (1) The uncertainties are more complex than what the Gaussian hypothesis states. (2) The independence of the two retrieval errors is not satisfied: even if the two retrievals are from two different instruments and wavelength (IR and MW), these uncertainties can be state-dependent which can introduce correlations among them. It is not a surprise that the weighted average is of better quality than the simple averaging because the uncertainty characterization for each source of information (even if it is not perfect) is taken into account: The weighted average will emphasize the observations with lower uncertainties.

Another striking comment is that the *a posteriori* combination can degrade the best independent retrieval! This can be observed for the $TCWV$ retrieval, with negative synergy factors observed (-6.64% and -1.88%). The simplistic mixture of the two independent retrievals can degrade the best one if the hypotheses are not correct, as already mentioned (Gaussian character and independence of the two retrieval errors). This could indicate a wrong individual uncertainty assessment, but the errors are well characterized in this example. This shows that the *a posteriori* combination is a too simplistic approach. For example, the individual retrieval uncertainties are dependent on the state of the atmosphere, so the weighting of the two independent retrievals should use such state-dependency.

	A posteriori combination				Data fusion
	Theoretical - Average	Retrieval - Average	Theoretical - Weighted	Retrieval - Weighted	Retrieval - NN TOTAL
RMS $TCWV$ (kg.m^{-2})	2.813	3.561	2.687	3.402	2.895
RMS TCO_3 (DU)	5.528	6.301	5.135	6.153	4.872
Synergy $TCWV$ (%)		-6.64		-1.88	13.29
Synergy TCO_3 (%)		4.35		6.60	26.04

TABLE 3. *A posteriori* combination versus data fusion retrieval statistics for $TCWV$ and TCO_3. For the *a posteriori* combination, both theoretical and real statistics are provided.

The comparison with the NN retrieval from the IR+MW configuration clearly shows that using simultaneously the two sources of information within the retrieval is much more performant than just combining *a posteriori* the individual retrievals. The synergy is much better exploited with the satellite data fusion principle. This should not be surprising (Aires 2011): Using simultaneously all the sources of information allows to add information[2] (i.e., additive synergy), reduce the uncertainties when the information is redundant (i.e., denoising synergy), but also, and this cannot be done with *a posteriori* combination, exploit the interaction terms (i.e., non-linear synergy). These non-linear interactions between the various input satellite observations makes it possible to account for the advantages and deficiencies of each satellite observation. For example, when a satellite observation is saturated for a particular range of the variable to retrieve, the other observations can help the retrieval. The NN data fusion is able to coherently combine the two sources of information (IR from IASI and MW from AMSU-A+MHS) in a way that depends upon the atmospheric situation.

6. Conclusion and perspectives

a. Conclusions

A retrieval chain has been designed to retrieve the atmospheric profiles from the MetOp-A satellite, exploiting the synergy between different measurements available from this operational platform. This satellite provides coincident observations in the IR, IASI and in the microwaves, AMSU-A and MHS, with nadir geometries. We concentrated this work on the major atmospheric parameters, namely temperature, water vapour and ozone profiles, for which the selected MetOp-A instruments are particularly sensitive. This work focused on clear-sky situations over ocean. The developed methodology is very general and flexible and can be adapted to other applications, i.e., other variables, instruments, or environmental conditions.

The results obtained here with real satellite observations confirm the theoretical results derived from simulations (Aires et al. 2011b). The major conclusions from this study are:

- The NN approach is very efficient to exploit the synergy due to its truly multivariate nature and its non-linear capacities (not all retrieval methodologies can benefit from the synergy between observations);
- Strong synergies exist between the microwave and the infrared for the retrieval of atmospheric temperature, water vapour and ozone. This synergy has been evidenced and quantified for the instruments on board the MetOp platform;
- Simple statistical retrieval tools can realistically measure the potential synergy of a set of satellite observations;
- The synergetic data fusion/merging of the satellite observations in the retrieval scheme is more performant than the *a posteriori* combination of products from independent retrievals.

Although the retrieval of atmospheric profiles under clear-sky conditions over ocean are already considered of reasonable quality when using one type of instrument only, the synergetic merging of the observations of different instrument improves the results. This study proves that there is still potential improvement in the retrieval of key atmospheric variables such as temperature, water vapour, or ozone profiles if synergy is used, even for supposedly "easy" conditions. The efficient use of simultaneous observations in various wavelength ranges makes it necessary to develop new retrieval strategies, as presented here. The variational assimilation developed in numerical weather prediction centers also benefits from the instrument synergy but if the goal is to obtain pure satellite datasets, to validate global circulation models for instance, methods have to be implemented to use the synergy among all available satellite observations. The NN approach proved its efficiency in this framework.

[2]If the summation is done optimally, with reliable assumptions.

b. Perspectives

The potential use of the synergy between the different observations opens exciting perspectives, the more difficult the problem, the higher the potential benefits of synergy. The visible information from the GOME II instrument is used to retrieve ozone profiles (Burrows et al. 2005). IASI also retrieves ozone (Aires et al. 2002; Coheur et al. 2005), and since we have shown that indirect synergy can also play so that MW observations can help the ozone retrieval, it would be very interesting to test the retrieval of ozone using the IR, MW and VIS synergy. Preliminary tests (not shown) indicate that the retrieval of ozone is very much improved when these three wavelength are used.

In this study, all observations were performed from the same platform. Note that the synergy between observations can also be applied to instruments on different platforms, although its practical application can be less convenient due to the necessity to have adequate spatial and temporal matching. The Sentinel suite would certainly benefit from the synergetic use of different observations from different satellites. We concentrated here on passive observations. Synergy can also be found between passive and active measurements at similar frequencies (this is the concept behind a mission such as Soil Moisture Active and Passive, SMAP).

In this first study, only ocean cases have been considered. The next natural step is to analyze the potential of using simultaneously IR and MW observations over the continents. In the MW as well as in the IR, several factors contribute to make retrieval of atmospheric profiles much more difficult over land than over ocean. First, surface temperatures and emissivities are much more variable in space and time over land than over ocean. Second, in the microwaves, the land surface emissivities are much higher than the ocean ones, making the surface contribution to the signal much larger. Finally, land surface emissivities are very complex to model, from arid surfaces to dense vegetation or snow, being dependant upon a large number of surface parameters that are difficult to estimate, on a global basis (e.g., soil moisture, soil roughness, lithology, snow cover and properties).

During the last years, several efforts have been conducted to develop global datasets of land surface emissivities at both microwave and infrared frequencies (Prigent et al. 2006; Seemann et al. 2008; Zhou et al. 2011), directly calculated from satellite observations. The use of *a priori* emissivity information has shown its potential to improve the retrieval of atmospheric parameters, namely water vapor and temperature over land, in research mode in the microwaves (Aires et al. 2001; Karbou et al. 2005; Aires et al. 2011b). Some work has also been done in the infrared (Seemann et al. 2008). A particularly interesting idea would be to combine the MW and the IR for the retrieval of atmospheric profiles over continents. Using all wavelength ranges will improve significantly the characterization of the surface, and the retrieval would benefit from a higher constrain in the inversion process, especially in the lower atmosphere. We suggest to extent the use of MW and IR observations from MetOp, for the retrieval of atmospheric profiles over land, with the help of the tools recently developed to estimate the land surface emissivities in the MW and in the IR.

Remote sensing under cloudy conditions would also certainly benefit from the synergy between the VIS, IR, and MW domains: First, the retrieval of cloud characteristics would benefit from the multi-wavelength observations (Aires et al. 2011a). Second, with clouds better constrained, the atmospheric retrieval would be facilitated. MW measurements are much less sensitive to clouds than the VIS and the IR, and to some extent, they can provide information in the clouds and below. Thin cirrus are essentially transparent at MW frequencies up to 200 GHz. Liquid clouds mostly interact with the MW radiation through emission/absorption and their effect can be accounted for rather simply in the retrieval of the atmospheric temperature and water vapor profiling. Convective clouds with a significant ice phase can scatter the MW radiation and their effect will be more difficult to take into account, likely limiting the accuracy of the profile retrieval. As a consequence, convective and precipitating situations should be avoided in a first attempt to evaluate the synergy of the VIS, IR and MW observations for atmospheric profiling (This could be the subject of later investigations). Under cloudy non-precipitating conditions, the MW, IR, and VIS measurements offer complementary information about the clouds. The IR provides its top height and its temperature. Preliminary information on the optical thickness of clouds can be derived from the VIS. Using simultaneously these different types of measurements will better constrain the inversion process and the retrieval will benefit from it. The inversion methodology developed for clear sky conditions over ocean can be adapted to the cloudy cases.

The synergy we evidenced in this study is very significant and should be taken into account in the design of the instruments for the new missions. The instrument characteristics should be determined not separately, independently for each sensor but instead, all the instruments should be taken into account, to optimize globally the whole observing system. The tools we developed in this study could be adopted to simulate the effect of the different potential channel characteristics and combinations to reach an optimum set of channels across wavelength ranges. This will not only ensure optimal retrieval accuracy, but also cost efficiency for the system, avoiding any non-necessary redundancies from an instrument to the other.

Acknowledgments.

This project has been funded by ESAs General Studies Programme (GSP) under contract "Towards a synergetic approach for the retrieval of atmospheric geophysical parameters from optical/infrared and microwave measurements", No 21837/08/NL/HE. We would like to express our gratitude to Björn Rommen and Marc Bouvet from ESA/ESTEC for interesting discussions related to this project.

REFERENCES

Aires, F., 2011: Measure and exploitation of multisensor and multi-wavelength synergy for remote sensing: Part i - theoretical considerations. *J. Geophys. Res.*, **116 (D02301)**, doi:10.1029/2010JD014701.

Aires, F., F. Bernardo, H. Brogniez, and C. Prigent, 2010: An innovative calibration method for the inversion of satellite observations. *JAMC*, **49 (12)**, 2458–2473.

Aires, F., F. Marquisseau, C. Prigent, and G. Sèze, 2011a: A land and ocean microwave cloud classification algorithm derived from amsu-a and -b, trained using msg-seviri infrared and visible observations. *Monthly Weather Rev., in press.*

Aires, F., M. Paul, C. Prigent, B. Rommen, and M. Bouvet, 2011b: Measure and exploitation of multi-sensor and multi-wavelength synergy for remote sensing: Part ii - an application for the retrival of atmospheric temperature and water vapour from metop. *J. Geophys. Res.*, **116 (D02303)**, doi:10.1029/2010JD014702.

Aires, F., C. Prigent, W. Rossow, and M. Rothstein, 2001: A new neural network approach including first-guess for retrieval of atmospheric water vapour, cloud liquid water path, surface temperature and emissivities over land from satellite microwave observations. *J. Geophys. Res.*, **106 (D14)**, 14 887–14 907.

Aires, F., W. B. Rossow, N. A. Scott, and A. Chédin, 2002: Remote sensing from the infrared atmospheric sounding interferometer instrument 2. Simultaneous retrieval of temperature, water vapor, and ozone atmospheric profiles. *Journal of Geophysical Research (Atmospheres)*, **107**, 7–1, doi:10.1029/2001JD001591.

Burrows, J., et al., 2005: The global ozone monitoring experiment (gome): Mission concept and first scientific results. *J. Atms. Sci.*, **56**, 151–175.

Chalon, G., F. Cayla, and D. Dievel, 2001: Iasi: an advanced sounder for operational meteorology. *Proceedings of the 52nd congress of IAF, Toulouse, France, 1-5 oct.*

Coheur, P., B. Barret, S. Turquety, D. Hurtmans, J. Lazaro, and C. Clerbaux, 2005: Retreival and characterization of ozone vertical profiles from a thermal infrared nadir sounder. *J. Geophys. Res.*, **110**, 418–439, doi:10.1029/2005JD005845.

Cybenko, G., 1989: Approximation by superpositions of a sigmoidal function. *Math. Control Signals Syst.*, **2**, 303–314.

Garand, L. and et Al., 2001: Radiance and jacobian intercomparison of radiative transfer models applied to hirs and amsu channels. *J. Geophys. Res.*, **106**, 24,017–24,031.

Hewison, T. and R. Saunders, 1996: Measurements of the amsu-b antenna pattern. *IEEE Trans. on Geoscience and Remote Sensing*, **34 (2)**, 405–412.

Hornik, K., M. Stinchcombe, and H. White, 1989: Multilayer feedforward networks are universal approximators. *Neural Networks*, **2**, 359–366.

Karbou, F., F. Aires, C. Prigent, and L. Eymard, 2005: Potential of amsu-a and -b measurements for atmospheric temperature and humidity profiling over land. *J. Geophys. Res.*, **110**, D07109, doi:10.1029/2004JD005318.

Mo, T., 1996: Prelaunch calibration of the advanced microwave sounding unit-a for noaa-k. *IEEE Trans. Microwave Theory and Techniques*, **44**, 1460–1469.

Prigent, C., F. Aires, and W. Rossow, 2006: Land surface microwave emissivities over the globe for a decade. *Bull. Amer. Meteor. Soc.*, 1572–1584, doi:10.1175/BAMS-87-11-1573.

Rumelhart, D., G. Hinton, and R. Williams, 1986: *Learning Internal Representations by Error Propagation*. MIT Press, Cambridge, 318-362 pp.

Seemann, S. W., E. E. Borbas, R. O. Knuteson, G. R. Stephenson, and H.-L. Huang, 2008: Development of a global infrared land surface emissivity database for application to clear sky sounding retrievals from multispectral satellite radiance measurements. *J. Appl. Meteorol. Clim.*, **47**, 108–123.

Smirnov, A., B. N. Holben, T. F. Eck, O. Dubovik, and I. Slutsker, 2000: Cloud-screening and quality control algorithms for the aeronet database. *Remote Sens. Environ.*, **73**, 337–349, doi:10.1016/S0034-4257(00)00109-7.

Zhou, D. K., A. M. Larar, X. Liu, W. L. Smith, L. L. Strow, P. Yang, P. Schlüssel, and X. Calbet, 2011: Global Land Surface Emissivity Retrieved From Satellite Ultraspectral IR Measurements. *Geoscience and Remote Sensing, IEEE Transactions on*, **49**, 1277–1290, doi:10..1109/TGRS.2010.2051036.